PLANT SCIENCE TODAY
Vol x(x): xx–xx
https://doi.org/10.14719/pst.13589

eISSN 2348-1900

RESEARCH ARTICLE

UPLC-QTOF-MS/MS-based metabolite profiling and regional bioactivity differences of *Codonopsis javanica* (Blume) Hook.f. & Thomson from Vietnam

Hoang Thu Thuy[1, 2], Ngo Thi Phuong[2*], Ta Thi Thao[1], Huijuan Cao[3], Do Thi Thanh Huyen[2] & Le Minh Ha[2*]

[1]Department of Chemistry, University of Science, Vietnam National University, Hanoi 100 000, Vietnam
[2]Institute of Chemistry, Vietnam Academy of Science and Technology (VAST), Ha Noi 100 000, Vietnam
[3]Beijing University of Chinese Medicine, Beijing 100 029, China

*Correspondence email - leminhha.inpc@gmail.com; ngophuong1688@gmail.com

Received: 09 January 2026; Accepted: 12 April 2026; Available online: Version 1.0: 31 May 2026

Cite this article: Hoang TT, Ngo TP, Ta TT, Huijuan C, Do TTH, Le MH. UPLC-QTOF-MS/MS-based metabolite profiling and regional bioactivity differences of *Codonopsis javanica* (Blume) Hook.f. & Thomson from Vietnam. Plant Science Today (Early Access). https://doi.org/10.14719/pst.13589

Abstract

The chemical composition and biological activities of roots of *Codonopsis javanica* (Blume) Hook.f. & Thomson collected from two distinct ecological regions of Vietnam (Kon Tum and Lai Chau Provinces) were investigated. Chemical profiling was performed using Ultra-performance liquid chromatography - Quadrupole Time-of-Flight - Tandem mass spectrometry (UPLC-QTOF-MS/MS)-based metabolite profiling (, while anti-inflammatory activity was evaluated via inhibition of nitric oxide (NO) production and immunomodulatory potential was assessed using phagocytosis-enhancing assays. A total of 35 metabolites belonging to major phytochemical classes, including saponin, phenolics, flavonoids, alkaloids, carboxylic acid, amino acids and other minor metabolites, were detected in *C. javanica,* of which 31 compounds are reported for the first time in *C. javanica*. Differences in metabolite profiles and related biological activities of *C. javanica* were observed between the two regions. Samples from Kon Tum Province showed stronger NO-inhibitory activity (IC_{50} = 84.69 µg/mL) and higher phagocytosis-enhancing activity (17.25 ± 1.59 %) than those from Lai Chau Province. These differences in bioactivity are likely attributable to variations in the levels of several key metabolites. The Kon Tum samples (CKT) contained higher amounts of syringin, lobetyolin, tangshenoside I, codonoside A and codonoside B compared with the Lai Chau samples (CLC), suggesting that these compounds play important roles in the biological activities of *C. javanica*. This is the first report combining UPLC-QTOF-MS/MS-based metabolite profiling with NO inhibition and phagocytosis-enhancing evaluations of *C. javanica*. The findings highlight the strong influence of ecological and climatic factors on the metabolic landscape and bioactivity of this medicinal plant.

Keywords: anti-inflammatory activity; *Codonopsis javanica*; immunomodulatory activity; metabolite profiling; MS-DIAL; UPLC-QTOF-MS/MS

Introduction

Codonopsis javanica (Blume) Hook.f. & Thomson is an important medicinal plant belonging to the Campanulaceae family and is widely distributed in the Northern mountainous regions and the Central highlands of Vietnam (1). This species has long been utilised in traditional medicine for restoring vitality, enhancing immunity and improving digestive function, owing to its abundant content of saponins, polysaccharides, flavonoids, organic acids and other secondary metabolites (2–3). The increasing demand for *C. javanica* in recent years has driven intensive harvesting across various ecological zones, among which Kon Tum (Ngoc Linh-Central Highlands) and Lai Chau (Hoang Lien Son - Northwest), which are considered as the two major natural distribution regions of the species (Fig. 1, 2). However, climatic and edaphic factors have been demonstrated to influence the accumulation of polysaccharides, total flavonoids and lobetyolin in *Codonopsis* (4). Based on this evidence, differences in the chemical composition of *C. javanica* from Kon Tum and Lai Chau can be expected and geographical factors may serve as chemical indicators for tracing the botanical origin of samples.



Fig. 1. Kon Tum *Codonopsis javanica.*



Fig. 2. Lai Chau *Codonopsis javanica.*

Several studies from China have successfully developed quality evaluation methods and discrimination models for *Codonopsis* radix based on chromatographic fingerprint analysis combined with chemometric approaches (SA, HCA, PCA and O2PLS-DA) and have identified characteristic marker compounds (including lobetyolin, syringin and tangshenoside I) for the differentiation of geographical origins (5–7). In addition, several studies have reported that the chemical composition of *Codonopsis* varies depending on the growth stage, cultivation conditions and harvesting conditions (8–10). The study showed that although root biomass of dangshen increased continuously, the contents of primary metabolites (polysaccharides, proteins) and secondary metabolites (phenolics, flavonoids) changed inversely with temperature and growth stage, suggesting a shift in carbon metabolism, with lobetyolin and atractylenolide III levels, indicating that autumn is the optimal harvest time (8). Additionally, repeated cultivation has significantly reduced the polysaccharide content in the roots (9). Studies on storage temperature have shown that *C. pilosula* roots stored at 9 °C maintain high respiratory intensity and elevated reactive oxygen species (ROS) levels, accompanied by a marked increase in malondialdehyde, indicating accelerated oxidative aging compared to other low-temperature conditions. Overall, multiple factors influence the quality of *Codonopsis* (10). However, in Vietnam previous studies on *Codonopsis*, particularly *C. javanica* mainly focused on qualitative assessment of major chemical groups or quantification of selected characteristic constituents such as total saponins, total sugars, polysaccharides, or marker compounds including lobetyolin (1, 11–13). Nevertheless, comprehensive comparative investigations of secondary-metabolite profiles between major harvesting regions such as Kon Tum and Lai Chau remain scarce. Meanwhile, the secondary metabolites of *C. javanica* exhibit high chemical diversity across multiple structural classes and their abundance is strongly influenced by geographical and ecological factors (4). Therefore, the traditional approach of analysing only a few quality markers becomes insufficient, particularly when the aim is to distinguish the geographical origin of the medicinal material.

Current trends in modern analytical chemistry emphasise the application of rapid, highly sensitive and high-resolution mass spectrometry techniques combined with advanced data-processing algorithms to construct holistic chemical profiles of herbal materials. Among these approaches, liquid chromatography - tandem mass spectrometry (LC-MS/MS) coupled with specialised data-processing platforms such as mass spectrometry-data independent analysis (MS-DIAL) has emerged as a powerful tool, enabling simultaneous screening of hundreds of compounds and rapid matching of MS/MS spectra with spectral libraries (14–17). Numerous studies applying LC-MS/MS in conjunction with MS-DIAL have demonstrated that plant chemical analysis becomes more comprehensive and objective, making this workflow particularly suitable for discriminating the geographical origin of medicinal materials based on metabolite profiling (11, 18–19).

Therefore, the present study aims to comparatively investigate the metabolite composition and biological activities of the roots of *C. javanica* collected from two regions of Vietnam using Ultra-performance liquid chromatography - Quadrupole Time-of-Flight - Tandem mass spectrometry-based metabolite profiling (UPLC-QTOF-MS/MS). The anti-inflammatory activity is evaluated via inhibition of nitric oxide (NO) production, while the immunomodulatory potential is assessed using phagocytosis-enhancing assays. Through the integration of metabolite profiling and bioactivity evaluation, this study sought to compare regional differences in chemical composition and biological effects of *C. javanica,* thereby providing further insight into the chemical basis underlying its bioactivities.

Materials and Methods

Plant materials

A total of 11 root samples of *C. javanica* were collected in November 2025, including 4 samples from Lai Chau province and 7 samples from the mountainous region of Kon Tum Province, Vietnam

Table 1. Information on samples

No	Voucher specimen code	Region	Harvest time
1	LC-MT-1	Muong Te -Lai Chau	11/2025
1.1	LC-MT-2	Muong Te - Lai Chau	11/2025
1.2	LC-SH-1	Sin Ho - Lai Chau	11/2025
1.3	LC-SH-2	Sin Ho - Lai Chau	11/2025
2	KT-T-1	Tumorong – Kon Tum	11/2025
2.1	KT-T-2	Tumorong – Kon Tum	11/2025
2.2	KT-T-3	Tumorong – Kon Tum	11/2025
2.3	KT-D-1	Dakglei – Kon Tum	11/2025
2.4	KT-D-2	Dakglei – Kon Tum	11/2025
2.5	KT-K-1	Konplong – Kon Tum	11/2025
2.6	KT-K-2	Konplong – Kon Tum	11/2025

(Table 1). The selected roots measured 6 cm to 15 cm in length and 0.3 cm to 1.5 cm in diameter, according to the Vietnamese Pharmacopoeia (20) (Table 1). The plant material was identified as *C. javanica* by Associate Professor Dr. Do Van Hai (Department of Botany, Institute of Biology, Vietnam Academy of Science and Technology) based on morphological characteristics in accordance with standard taxonomic references (21).

After collecting, the samples were dried at 70 °C, then finely ground and passed through a 355-mesh sieve to obtain homogeneous powdered material. The resulting powder was stored in a clean sample bottle, sealed and labeled (22).

Chemical materials

Ethanol 96 %, nitroblue tetrazolium (NBT) dye; 96-well plastic microplates (Corning, USA), pipettes (Eppendorf) and a 96-well ELISA microplate reader (BioTek); the RAW264.7 cell line provided by Professor Domenico V Delfino, University of Perugia, Italy; Murine macrophage RAW264.7 cell line (American Type Culture Collection, ATCC, Manassas, VA, USA); Dulbecco's Modified Eagle Medium (DMEM; Thermo Fisher Scientific, Waltham, MA, USA); Fetal bovine serum (FBS; Thermo Fisher Scientific, Waltham, MA, USA); Lipopolysaccharide (LPS; Merck KGaA, Darmstadt, Germany); MTT reagent (3-(4,5-dimethylthiazol-2-yl)-2,5-diphenyltetrazolium bromide; Merck KGaA, Darmstadt, Germany); Griess reagent (Merck KGaA, Darmstadt, Germany); Sodium nitrite ($NaNO_2$; Merck KGaA, Darmstadt, Germany); Cardamonin (Sigma-Aldrich, St. Louis, MO, USA); Dimethyl sulfoxide (DMSO; Sigma-Aldrich, St. Louis, MO, USA); Phosphate-buffered saline (PBS; Thermo Fisher Scientific, Waltham, MA, USA).

Extraction

A total of 50 g of powdered material was extracted with 300 mL of an ethanol-water mixture (7:3, v/v) at 50 °C for 2 hr (23). The extract was then allowed to cool to room temperature and filtered using a

vacuum filtration system to obtain the *C. javanica* root extract. The filtrate was concentrated to dryness, after which the residue was re-dissolved and brought to a final volume of 100 mL with the same ethanol-water solvent system (7:3, v/v). The solution was subsequently filtered through a 0.22 µm PTFE membrane into 2 mL vials prior to UPLC-QTOF-MS/MS analysis (23). A quality control (QC) sample was prepared by mixing equal volumes of one randomly selected sample from Kon Tum and one from Lai Chau.

UPLC-QTOF-MS/MS analysis

UPLC-QTOF-MS analysis was performed on an ExionLC™ UPLC system (SCIEX, USA) coupled to an X500B QTOF tandem mass spectrometer (SCIEX, USA). Chromatographic separation of the *C. javanica* extracts was achieved on a C18 110 Å column (2.0 × 50 mm, 3 µm) using a mobile phase consisting of solvent A (water containing 0.1 % formic acid) and solvent B (methanol containing 0.1 % formic acid) under the following gradient program: 0–2 min, 10 % B; 2–7 min, 50 % B; 7–12 min, 10 % B. The column temperature is maintained at 30 °C. The flow rate was set at 0.3 mL/min and the injection volume was 2 µL (23).

Mass spectrometric detection was conducted in both positive and negative electrospray ionisation modes. The TOF-MS acquisition was carried out over an m/z range of 100–1500 Da, with a declustering potential of 50 V (-80 V in negative mode), collision energy of 15 V and accumulation time of 0.1 sec. For TOF-MS/MS acquisition, the m/z range was set to 50–1500 Da, the declustering potential was maintained at 50 V (-80 V for negative mode), the collision energy was 30 V and the accumulation time was 0.05 sec. Nebuliser gas pressure was 50 psi, drying gas 50 psi and the source temperature was 500 °C. Mass accuracy was calibrated using the Calibration Solution Mix (P/N: 4460131) supplied by the manufacturer. Mass calibration was performed after every five measurements.

Chemical identification using MS-DIAL

The MS/MS spectra of one blank sample, eleven *C. javanica* samples and one QC sample were converted from the original .wiff2 format to .mzML using the MSConvert software. The processed data were then imported into MS-DIAL version 5.5 for compound annotation through spectral matching against reference databases. Chromatograms and mass spectra of all samples were aligned to the QC sample to correct retention time shifts and m/z deviations. MS/MS-based compound annotation was performed using MS-DIAL by matching the experimental spectra against the MoNA-export spectral libraries, including All_LC-MS/MS_QTOF and MassBank. In addition, the MS-FINDER tool integrated into the MS-DIAL software was also employed to perform *in silico* structural elucidation in cases where certain suspected ions could not be identified through matching with available spectral databases. The accurate mass tolerance was set to 0.01 Da for both precursor ions (MS1) and fragment ions (MS2), while the retention time tolerance was fixed at 0.05 to 0.1 min. The mass range for fragment ions was defined from 0 to 1500 Da. Spectral matching was accepted when the following criteria were simultaneously fulfilled: dot product score ≥ 750, weighted dot product score ≥ 750, reverse dot product score ≥ 600, matched spectrum percentage ≥ 25 % and a minimum of three matched fragment ions. These thresholds were selected to ensure reliable compound annotation based on MS/MS spectral similarity.

The dataset of QC sample was selected as the reference file. The retention time tolerance was 0.1 min, with MS1 and MS2 mass tolerances of 0.015 and 0.025 Da, respectively. Blank-based feature removal was enabled using the criterion of sample maximum to blank average ratio, with a fold-change threshold of 5. Features removable based on blank information were retained and tagged. Gap filling by compulsion was enabled to improve data completeness across samples, while reference-matched and MS2-unsuggested metabolite features were not forcibly retained. The MS-DIAL workflow was validated using pooled QC samples. Mass accuracy and retention time (RT) repeatability were evaluated after five injections. Features were retained when present in ≥ 80 % of QC injections, with RT deviation ≤ 0.1 min and MS1 mass error ≤ 5 ppm.

Evaluation of the anti-inflammatory activity of *Codonopsis javanica* extracts

Equal amounts of powdered herbal material were pooled within each group: seven *C. javanica* samples from Kon Tum (CKT) and four *C. javanica* samples from Lai Chau (CLC), resulting in two pooled samples, designated as CKT-M and CLC-M respectively and extraction was carried out as described in the extraction section. The resulting extracts were concentrated to a viscous residue and subsequently dried in a drying oven at 65 °C to obtain solid extracts with a moisture content of less than 5 %.

The anti-inflammatory activity of the CKT-M and CLC-M extracts was evaluated using the RAW 264.7 murine macrophage cell model (24). RAW 264.7 cells were cultured for 48 hr in DMEM supplemented with 10 % FBS (fetal bovine serum) at 37 °C in a humidified atmosphere containing 5 % CO_2 (25, 26). The cells were then seeded into 96-well plates at a density of 2.5 × 105 cells per well. Inflammation was induced by lipopolysaccharide (LPS) stimulation for 24 hr, followed by treatment with the test samples at concentrations ranging from 256 to 16 µg/mL. Cardamonin was used as the positive control. The cell culture supernatant was reacted with Griess reagent and sodium nitrite ($NaNO_2$) solutions at different concentrations were used to construct a calibration curve. The absorbance was measured at a wavelength of 570 nm. The inhibition rate of nitric oxide (NO) production (%) was calculated as follows:

$$NO(\%) = \frac{[\bar{X}]_{sample} - [\bar{X}]_{LPS}}{[\bar{X}]_{control} - [\bar{X}]_{LPS}} \times 100 \qquad \text{(Eqn. 1)}$$

In which $[\bar{x}]$ represents the mean NO concentration calculated based on the $NaNO_2$ calibration curve.

To evaluate the *in vitro* cytotoxicity of the samples, cells under the same experimental conditions were treated with MTT solution (0.5 mg/mL in PBS) and incubated for 4 hr in a humidified incubator at 37 °C with 5 % CO_2. The resulting formazan crystals were dissolved in dimethyl sulfoxide (DMSO, Sigma-Aldrich) and the absorbance was measured at 540/720 nm using a Tecan Spark microplate reader (Männedorf, Switzerland). The cell survival rate (CS %) was calculated as a percentage of optical density (OD) relative to the negative control (–):

$$CS\,\% = \frac{OD_{sample}}{OD_{negative\ quality\ (-1)}} \times 100 \pm \sigma \qquad \text{(Eqn. 2)}$$

Where σ represents the standard deviation:

$$\sigma = \sqrt{\frac{\sum(x_i - \bar{x})^2}{n-1}} \qquad \text{(Eqn. 3)}$$

Evaluation of the phagocytosis-enhancing activity of *Codonopsis javanica* extract

Murine macrophage RAW 264.7 cells were cultured in Dulbecco's Modified Eagle Medium (DMEM) supplemented with 2 mM L-glutamine, 10 mM HEPES and 1.0 mM sodium pyruvate and further enriched with 10 % fetal bovine serum (FBS) (GIBCO). The cells were maintained in a humidified CO_2 incubator at 37 °C under 5 % CO_2 atmosphere. Cells were seeded into 96-well plates at an appropriate density in 190 µL of culture medium per well and incubated overnight at 37 °C to allow cell attachment and stabilisation.

CKT-M and CLC-M 10 µL were prepared in 10 % DMSO, were added to the wells at different concentrations. A separate 96-well plate containing cells (190 µL) with 10 µL DMSO (0.1 %) but without test samples was used as the negative control. After 2 hr of incubation, lipopolysaccharide (LPS) was added to selected wells at a final concentration of 10 µg/mL.

Phagocytic activity of macrophages is commonly associated with the generation of ROS and can be evaluated using the nitroblue tetrazolium (NBT) reduction assay (27). A higher degree of NBT reduction corresponds to increased oxidase enzyme activity and thus reflects enhanced phagocytic stimulation. The NBT dye reduction assay was performed using the standard RAW 264.7 macrophage cell line to assess phagocytic activity.

Briefly, 20 µL of cell suspension and 40 µL of Roswell park memorial institute (RPMI) medium were added to each well of a 96-well plate. Subsequently, 20 µL of the test samples at various concentrations were introduced into the experimental wells. The sample solvent was used as the negative control. After 24 hr of incubation, 20 µL of heat-inactivated yeast cell suspension (*Saccharomyces cerevisiae*) and 20 µL of NBT solution (Sigma) were added to each well and incubated at 37 °C. After 60 min, wells containing adherent macrophages were washed with RPMI medium and subsequently washed four times with 200 µL methanol. Following air-drying, 120 µL of 2 M KOH and 140 µL of DMSO were added. Absorbance was measured using a microplate spectrophotometer (BioTek) at a wavelength of 570 nm and the percentage of NBT reduction was calculated according to the following formula:

$$\% \text{ NBT reduction} = \frac{\text{OD (sample)} - \text{OD (negative control)}}{\text{OD (negative control)}} \times 100\ \% \quad \text{(Eqn. 4)}$$

All experiments were performed in triplicate. Data were expressed as mean ± standard deviation (SD). Statistical analysis was performed using one-way analysis of variance (ANOVA), followed by Dunnett's test to compare each treated group with the control. Differences were considered statistically significant at $p < 0.05$.

Results and Discussion

Identification of compounds in *Codonopsis javanica*

Compounds were identified by matching the aligned MS/MS spectra of the samples with those in the reference database, followed by filtering based on a match score threshold (≥ 1.8) (28), MS1 mass accuracy for QTOF-MS/MS instruments (≤ 5 ppm) (29) and a minimum peak signal-to-noise ratio of > 10. In total, 24 compounds in positive ion mode and 11 compounds in negative ion mode were identified (Table 2). The MS/MS fragmentation spectra of the compounds are presented in Supplementary Table 1.

Alkaloids

In the MS/MS spectrum, trigonelline produces a [M+H]+ ion at m/z = 138.055, which preferentially undergoes loss of HCOOH from its carboxylate moiety to form the N-methylpyridinium ion $[C_6H_6N]$+ at m/z = 92.0500. Subsequent cleavage of HCN yields the fragment ion $[C_5H_5]$ at m/z = 65.0391 along with lower-mass fragments. Norharman exhibits an MS/MS spectrum characterised by a precursor ion at m/z = 169.0765 and fragment ions $[C_{10}H_8N]$+, $[C_6H_5C_3H_2]$+ and $[C_7H_5]$+ appearing at m/z = 142.0657, 115.0547 and 89.0388 respectively. This compound has previously been reported in root extracts of *C. lanceolata* (30). Harmane produces MS/MS fragments at m/z = 168.0686, 142.0658 and 115.0546, corresponding to neutral losses of -CH_3, -CH_3N and -$C_3H_4N_2$ respectively. Similar to norharman, this compound has also been detected in root extracts of *C. lanceolata* (30). Berberine yields characteristic MS/MS fragments at m/z = 292.0972 and 262.0831, attributable to successive losses of two -CH_3 groups and an -OCH_2 substituent. Columbamine displays diagnostic fragments at m/z = 322.1070 and 294.1124, consistent with cleavage of -CH_3 and -OCH_3 groups. The most intense fragment, observed at m/z = 240.2317, reflects the combined loss of -$N(CH_3)_3$ and -COOH functionalities.

Amino acids

Aspartic acid exhibits an MS/MS spectrum characterised by fragments at m/z = 88.0410 and 71.0135, corresponding to the ions $[C_3H_6NO_2]$+ and $[C_3H_3O_2]$+ respectively, indicative of cleavages involving the -COOH and -NH_2 groups. This amino acid has been reported in the roots of *C. pilosula* at concentrations ranging from 2.21 to 2.54 mg/g (31). Glutamic acid presents diagnostic MS/MS fragments at m/z = 128.0329 and 102.0564, assigned to the ions $[C_5H_6NO_3]$- and $[C_4H_8NO_2]$-, reflecting neutral losses of -OH and the -COOH group. According to a previous study, its concentration in *C. pilosula* ranges from 4.05 to 13.54 mg/g (31). In the MS/MS spectrum, 4-guanidino-butanoate generates a [M+H]+ ion at m/z = 146.0926 and undergoes preferential cleavage adjacent to the guanidino moiety to yield the characteristic guanidinium ion $[C(NH_2)_3]$+ at m/z = 86.0604. Phenylalanine produces a prominent fragment ion $[C_6H_5C_2H_5N]$+ at m/z = 120.0809, followed by loss of NH_3 to form the ion $[C_8H_7]$+ at m/z = 103.0542. The fragment at m/z = 77.0386 represents the phenyl cation $[C_6H_5]$+, confirming the presence of the aromatic ring. Arginine shows a precursor ion at m/z=175.1192, with a key fragment at m/z = 116.0714 corresponding to $[C_5H_{10}NO_2]$+, arising from cleavage of the $[CN_3H_4]$+ group. The fragment at m/z = 70.0655 corresponds to $[C_4H_8N]$+. This amino acid has been quantified at 5.47–23.29 mg/g in *C. pilosula* roots collected in China (31). Tyrosine produces MS/MS fragments at m/z = 165.0554, 136.0761 and 119.0496, representing losses of -NH_2 and -COOH. The ion at m/z 91.0546 corresponds to $[C_6H_5CH_2]$+, characteristic of a benzyl fragment. Tryptophan yields diagnostic fragments at m/z = 188.0711, 170.0607 and 146.0606, associated with losses of -NH_3, -OH and -CH_3 respectively. The fragment at m/z = 118.0657 corresponds to the indole-derived ion $[C_6H_4C_2H_3HN]$+. This compound has been reported at levels of 0.8–1.1 mg/g dry weight in the roots of *C. pilosula* (Franch.) Nannf (32, 33) and has been isolated from *C. javanica* (34).

Table 2. Annotated compounds identified in the *Codonopsis javanica* samples

No	Rt (min)	m/z (Da)	Metabolite name	Adduct type	Formula	Error (ppm)
			Alkaloids			
1	1.48	138.0549	Trigonelline	[M+H]+	$C_7H_7NO_2$	-0.14
2	5.13	169.0765	Norharman	[M+H]+	$C_{11}H_8N_2$	2.54
3	5.27	183.0919	Harmane	[M+H]+	$C_{12}H_{10}N_2$	1.42
4	6.37	336.1216	Berberine	[M]+	$C_{20}H_{18}NO_4$	-4.91
5	5.93	338.1383	Columbamine	[M]+	$C_{20}H_{20}NO_4$	-1.6
			Amino acids			
6	1.30	132.0302	Aspartic acid	[M-H]-	$C_4H_7NO_4$	-0.08
7	1.33	146.0459	Glutamic acid	[M-H]-	$C_5H_9NO_4$	0.27
8	1.89	146.0924	4-guanidino-butanoate	[M+H]+	$C_5H_{11}N_3O_2$	-2.81
9	4.46	166.0859	Phenylalanine	[M+H]+	$C_9H_{11}NO_2$	-2.29
10	1.31	175.1189	Arginine	[M+H]+	$C_6H_{14}N_4O_2$	-4.17
11	1.93	182.081	Tyrosine	[M+H]+	$C_{-9}H_{11}NO_3$	-4.45
12	4.76	205.0979	Tryptophan	[M+H]+	$C_{11}H_{12}N_2O_2$	-2.19
			Carbohydrates			
13	1.44	179.0561	Galactose	[M-H]-	$C_6H_{12}O_6$	-0.11
14	1.31	181.0717	D-mannitol	[M-H]-	$C_6H_{14}O_6$	-0.44
15	1.44	341.1086	Sucrose	[M-H]-	$C_{12}H_{22}O_{11}$	-0.97
			Carboxylic acid			
16	6.03	187.0969	Azelaic acid	[M-H]-	$C_9H_{16}O_4$	-3.74
17	1.49	191.0194	Citric acid	[M-H]-	$C_6H_8O_7$	-1.62
18	1.4	191.0561	Quinic acid	[M-H]-	$C_7H_{12}O_6$	-0.21
19	1.32	195.0507	Gluconic acid	[M-H]-	$C_6H_{12}O_7$	-1.79
			Flavonoids			
20	7.32	257.0811	Liquiritigenin	[M+H]+	$C_{15}H_{12}O_4$	-5.1
21	6.54	301.0352	Quercetin	[M-H]-	$C_{15}H_{10}O_7$	-0.66
22	6.11	431.1344	Calycosin-7-O-beta-D-glucoside	[M+H]+	$C_{22}H_{22}O_9$	1.62
			Phenolics			
23	4.56	109.0292	Catechol	[M-H]-	$C_6H_6O_2$	-2.57
24	9.25	245.1167	Osthol	[M+H]+	$C_{15}H_{16}O_3$	-2.24
25	4.8	395.132	Syringin	[M+Na]+	$C_{17}H_{24}O_9$	-1.47
26	5.34	419.1669	Lobetyolin	[M+Na]+	$C_{20}H_{28}O_8$	-1.74
27	5.58	847.2629	Codonoside B	[M+Na]+	$C_{38}H_{48}O_{20}$	-0.25
28	5.70	847.2643	Codonoside A	[M+Na]+	$C_{38}H_{48}O_{20}$	1.33
			Saponin			
29	4.87	701.228	Tangshenoside I	[M+Na]+	$C_{29}H_{42}O_{18}$	2.32
			Lipids			
30	1.39	258.1106	Sn-glycero-3-phosphocholine	[M+H]+	$C_8H_{20}NO_6P$	1.78
31	8.51	318.2999	Phytosphingosine	[M+H]+	$C_{18}H_{39}NO_3$	-1.32
			Other compounds			
32	1.91	123.0548	Nicotinamide	[M+H]+	$C_6H_6N_2O$	-3.82
33	4.81	127.039	3-hydroxy-2-methyl-4-pyrone	[M+H]+	$C_6H_6O_3$	-0.08
34	9.23	184.0736	Phosphorylcholine	[M+H]+	$C_5H_{14}NO_4P$	1.41
35	7.63	343.2954	Lauramidopropyl betaine	[M]+	$C_{19}H_{39}N_2O_3$	-0.35

Carbohydrates

The MS/MS spectrum of galactose displays fragment ions at m/z = 89.0225, 71.0143 and 59.0142, corresponding to $[C_3H_5O_3]$- and $[C_3H_3O_2]$-. This monosaccharide has also been reported as a structural component of the pectic polysaccharide CPP1b isolated from *C. pilosula* (35). D-Mannitol yields diagnostic MS/MS fragments at m/z = 101.0260, 89.0242 and 71.0139, assigned to $[C_4H_5O_3]$-, $[C_3H_5O_3]$- and $[C_3H_3O_2]$- respectively, reflecting sequential cleavages of -OH and -CH groups within the molecule. The MS/MS spectrum of sucrose features a prominent fragment at m/z = 179.0562, corresponding to $[C_6H_{11}O_6]$- and characteristic of the glucose ring. Additional ions at m/z = 131.0581, $[C_5H_7O_4]$- and 89.0241, $[C_3H_5O_3]$- further support its fragmentation behaviour. Sucrose is known to be a major sweetening sugar in the roots of *Codonopsis* species (36).

Carboxylic acid

Azelaic acid exhibits characteristic MS/MS fragments at m/z = 169.0856, 143.1075 and 125.097, corresponding to successive losses of –OH and –COOH groups. This compound has been reported in the roots of *C. radix* (37). Citric acid produces a diagnostic fragment at m/z = 111.0094, assigned to $[C_5H_3O_3]$-, indicative of decarboxylation. The compound has been identified in *C. ussuriensis* using LC-QTOF-MS (38). Quinic acid shows MS/MS ions at m/z = 173.0459, reflecting loss of -OH and at m/z = 127.0406, $[C_6H_7O_3]$-, corresponding to decarboxylation. Quinic acid derivatives have been reported in the aerial parts of *C. canescens* and *C. nervosa* (39). Gluconic acid yields MS/MS fragments at m/z = 129.019, 99.0092 and 75.0088, corresponding to $[C_5H_5O_4]$-, $[C_4H_3O_3]$- and $[C_2H_3O_3]$-, consistent with cleavages of -C-OH groups. It is one of the sweetness-contributing components previously documented in *C. canescens* Nannf. and C. *nervosa* Nannf. from Tibet, China (39).

Flavonoids

Liquiritigenin produces MS/MS fragments at m/z = 211.0759, corresponding to $[C_{14}H_{10}O_2]$+ formed by losses of -OH and -CO. The fragment at m/z = 137.0235, assigned to $[C_7H_5O_3]$+, further supports its characteristic cleavage pattern. Quercetin, a flavonoid reported in *Codonopsis* radix yields diagnostic ions at m/z = 245.0460, 151.0032 and 121.0284, corresponding to $[C_{13}H_9O_5]$-, $[C_7H_3O_4]$- and $[C_7H_5O_2]$-, respectively (40). Calycosin-7-O-beta-D-glucoside exhibits a prominent fragment at m/z = 269.0807, $[C_{16}H_{13}O_4]$+, indicative of glucose moiety cleavage.

Phenolics

Catechol exhibits an MS/MS spectrum with fragment ions at m/z = 91.0187, 80.0286 and 53.0401, corresponding respectively to $[C_6H_3O]$-, $[C_5H_4O]$- and $[C_4H_5]$-, which are characteristic of a benzene-ring fragmentation pattern. Osthol presents diagnostic MS/MS fragments at m/z = 189.0548, assigned to the $[C_{11}H_9O_3]$+ ring system and m/z = 131.0492, corresponding to $[C_9H_7O]$+, indicative of ring cleavage adjacent to the -O- bond. Syringin is detected in the form of [M+Na]+, with a precursor ion at m/z = 395.1317 and a major product ion at m/z = 233.0785, corresponding to $[C_{13}H_{13}O_4]$+, reflecting successive losses of -OH groups and cleavage of the glucose moiety. Lobetyolin was identified using MS-FINDER in the form of the [M+Na]+ ion. The MS/MS spectrum of the molecular formula proposed by MS-FINDER showed a fragment at m/z = 241.1217, corresponding to $[C_{14}H_{18}O_2Na]$+, indicating cleavage of the glycosidic moiety and a fragment at m/z 203.0536 corresponding to the glycosidic ring $[C_6H_{12}O_6Na]$+. These fragment ions are characteristic of lobetyolin and have been reported in several previous studies (37, 41). Syringin and lobetyolin have been previously isolated from *C. javanica* (34). Codonoside A and codonoside B, with precursor ions detected as [M+Na]+, exhibited similar MS/MS fragmentation patterns. A fragment at m/z = 655.1843, corresponding to the ion $[M+Na–C_{11}H_{12}O_3]$+, indicated cleavage at the linkage between the glycosidic moiety and the $CH_3OC_6H_4CHCOO$- side chain, while the fragment at m/z = 493.1313 was assigned to the characteristic ion $[C_{21}H_{26}O_{12}Na]$+. The chromatographic peaks of the two codonosides were not completely resolved; therefore, based on previous studies, the peak at RT = 5.58 min was assigned to codonoside B, whereas the peak at RT = 5.70 min was assigned to codonoside A (37). Both compounds were identified using the MS-FINDER tool.

Saponin

Tangshenoside I exhibited an MS/MS spectrum with a characteristic fragment ion at m/z=347.0949, corresponding to $[C_{14}H_{19}O_{10}]$+, which is indicative of cleavage at the -CH=CH- double bond linking the syringin moiety with the meglutol glucoside unit. Tangshenoside I is one of the representative saponins in *Codonopsis* radix and is regarded as a biological marker for discriminating *Codonopsis* samples of different geographical origins (31). This compound has been isolated from *C. javanica* (42).

Lipids

Sn-glycero-3-phosphocholine exhibits an MS/MS spectrum featuring a fragment at m/z = 125.0002, corresponding to $[C_2H_6O_4P]$+, which is diagnostic of the sn-glycero-3-phosphocholine backbone. Phosphorylcholine displays characteristic MS/MS fragments at m/z = 125.0029 and 86.0971, assigned to $[C_5H_4NOP]$+ and $[C_5H_{12}N]$+ respectively, consistent with the structural features of this compound.

Other compounds

In the MS/MS spectrum of nicotinamide, the [M+H]+ ion (m/z = 123.0556) undergoes cleavage at the bond between the pyridine ring and the carboxamide group, producing the pyridinium ion $[C_5H_5NH]$+ at m/z = 80.049. Nicotinamide, an amide derivative of niacin (vitamin B_3), has been reported to accumulate predominantly in the leaves compared with the stems and roots of *C. convolvulacea* (29). 3-Hydroxy-2-methyl-4-pyrone generates an [M+H]+ ion at m/z = 127.0396, followed by fragmentation around the C=O–C(OH)= moiety and the CH_3 substituent. Subsequent ring opening and rearrangement yield low-mass diagnostic fragments such as m/z = 53.0400 ($[C_4H_5]$+) and m/z = 43.0180 ($[C_2H_3O]$+). Phytosphingosine exhibits diagnostic MS/MS fragments at m/z = 282.2793, indicative of -OH group cleavage and m/z = 60.0449, characteristic of the $[C_2H_6NO]$+ moiety.

Using UPLC–QTOF-MS/MS, a total of 35 compounds were detected in the roots of *C. javanica* cultivated in Vietnam. Among these, 31 compounds have not been previously reported in *C. javanica,* covering alkaloids (trigonelline, norharman, harmane, berberine and columbamine), amino acids (aspartic acid, glutamic acid, 4-guanidino-butanoate, phenylalanine, arginine and tyrosine), carbohydrates (galactose, D-mannitol and sucrose), carboxylic acids (azelaic acid, citric acid, quinic acid and gluconic acid), flavonoids (liquiritigenin, quercetin and calycosin-7-O-β-D-glucoside), phenolic compounds (catechol, osthol, codonoside A and codonoside B),

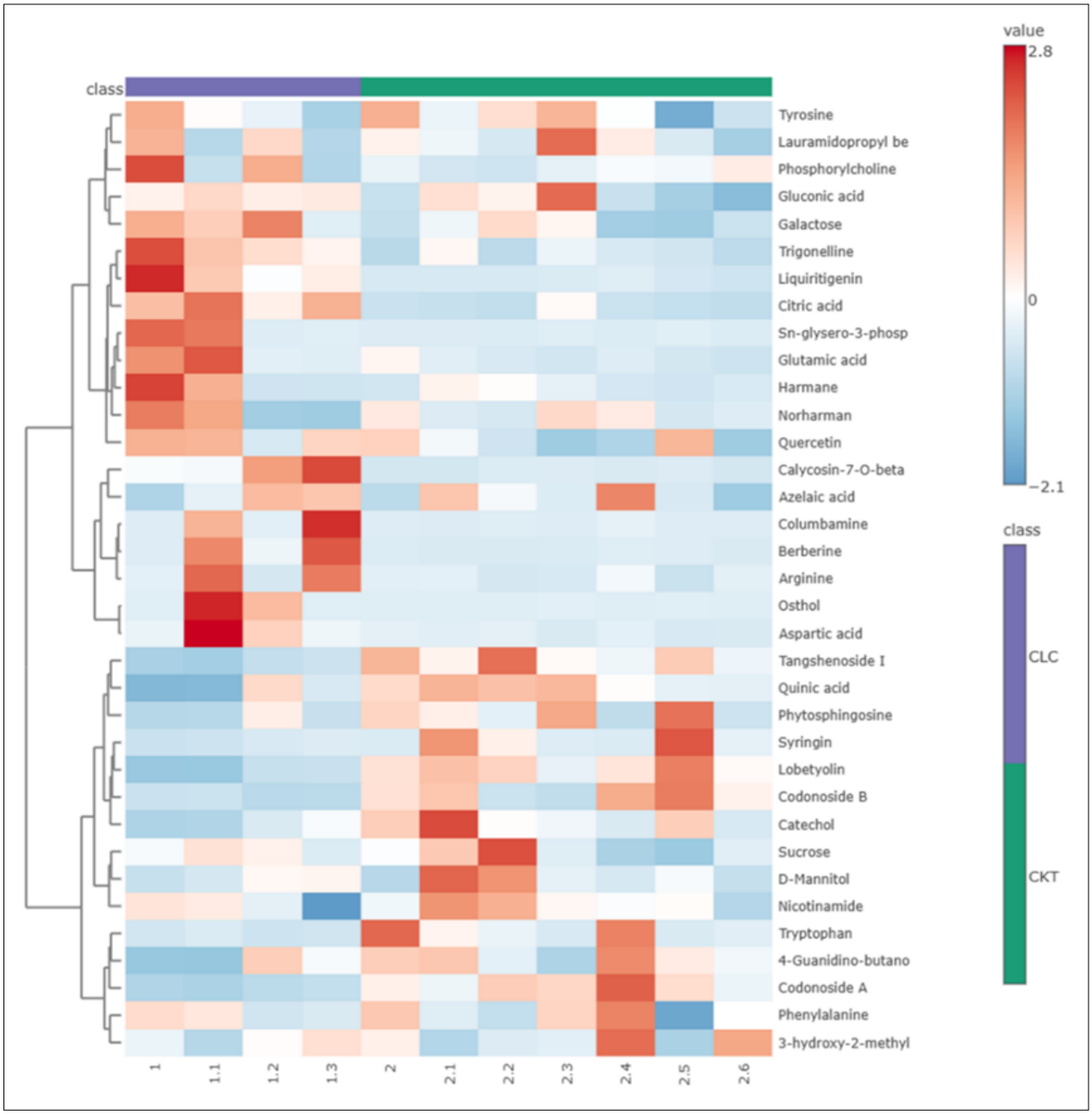


Fig. 3. Heatmap of peak areas for annotated compounds in CKT and CLC samples.

lipids (sn-glycero-3-phosphocholine and phytosphingosine) and several other metabolites, including nicotinamide, 3-hydroxy-2-methyl-4-pyrone, phosphorylcholine and lauramidopropyl betaine.

Preliminary classification of samples from Lai Chau and Kon Tum (Vietnam)

In this study, peak-area data of annotated metabolites in four CLC and seven CKT sample were visualised using heatmap analysis generated via the MetaboAnalyst platform. Differences between the two groups were evaluated using the Welch's t-test. To account for multiple comparisons across annotated compounds, p-values were adjusted using the Benjamini–Hochberg procedure and results with adjusted p-values (FDR) < 0.05 were considered statistically significant. Hierarchical clustering analysis (HCA) and heatmap visualisation were performed using Euclidean distance and Ward's linkage method to assess the relative abundance patterns of metabolites across samples (Fig. 3).

The heatmap reveals a clear separation between the two *C. javanica* sample groups based on UPLC–QTOF-MS/MS profiling, reflecting distinct patterns in the accumulation of primary and secondary metabolites across ecological regions. Overall, CLC samples exhibit higher signal intensities for most amino acids (aspartic acid, glutamic acid, arginine) and alkaloids (trigonelline, columbamine, harmane, norharmane, berberine), whereas CKT samples show elevated levels of phenolic compounds (syringin, lobetyolin, catechol, codonoside A, codonoside B), saponin (tangshenoside I) and carbohydrates (galactose, sucrose, D-mannitol).

According to previously published studies, temperature exerts a significant positive correlation with the accumulation of soluble sugars, whereas precipitation shows a negative correlation with the accumulation of tangshenoside I. In addition, soil sand content is negatively correlated with syringin levels (43). We examined the annual precipitation and temperature data for 2023 and 2024 in the two regions of Kon Tum and Lai Chau (Fig. 4, 5). Overall, the statistics indicate that average precipitation in Kon Tum was higher than that in Lai Chau during the summer–autumn months, whereas during the winter–spring period, precipitation in Kon Tum was lower than in Lai Chau. In contrast, the mean annual temperature in Kon Tum was higher than that in Lai Chau, while the temperature amplitude was lower (44). We also considered the soil

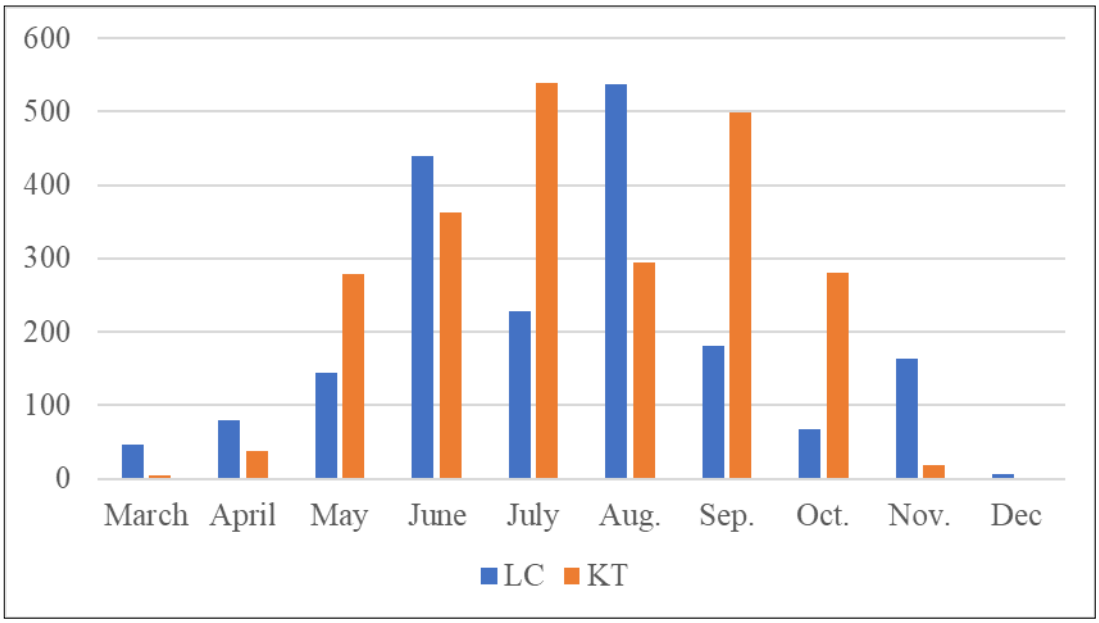


Fig. 4. Average monthly rainfall in Lai Chau and Kon Tum from March–December 2023.

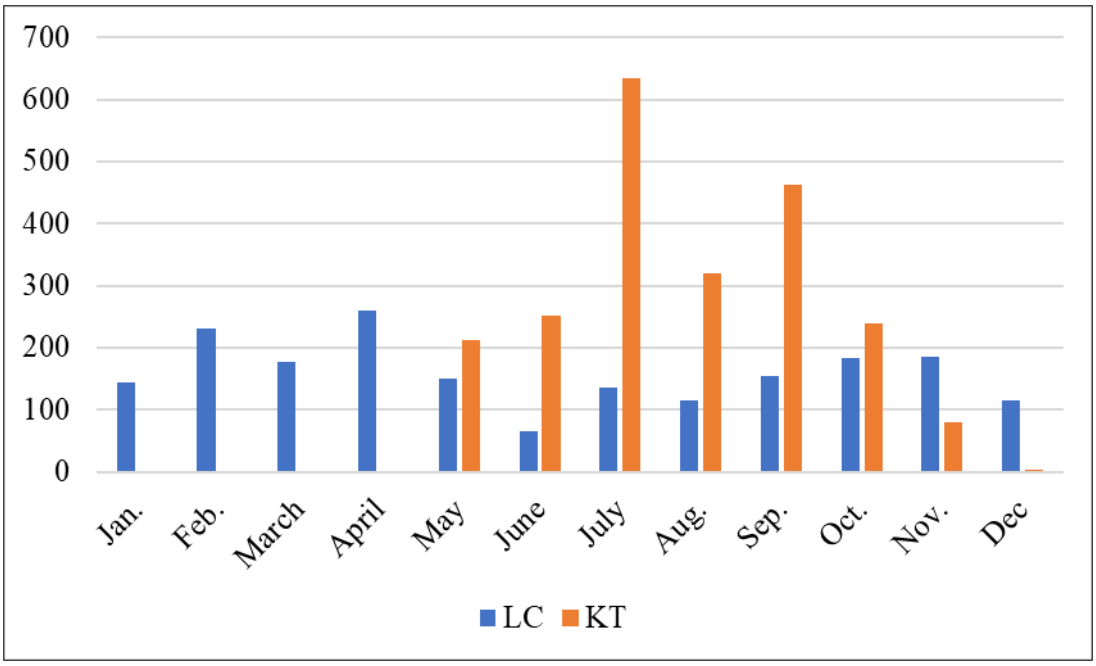


Fig. 5. Average monthly rainfall in Lai Chau and Kon Tum on 2024.

conditions in Kon Tum, where the soil is mainly red basalt, rich in nutrients and has a lower sand content compared to the red-yellow ferralitic soil in the Lai Chau (45). Under these environmental conditions and considering the harvesting period in November, the CKT samples appeared to contain relatively higher levels of soluble sugars, tangshenoside I and syringin than the CLC samples. This observation is broadly consistent with the trends reported in a previous study (43). In addition, Kon Tum is located at an elevation of approximately 1600 m, whereas the Lai Chau sampling sites are situated at around 600 m above sea level. Differences in altitude may represent one of several environmental factors that influence the accumulation of chemical constituents in *Codonopsis* (46).

Syringin, lobetyolin and tangshenoside I have been widely recognised as potential marker compounds for the authentication and quality evaluation of *Codonopsis* species (7, 41). In the present study, these three compounds exhibited pronounced differences in abundance between the CLC and CKT samples, highlighting their suitability as key discriminators for differentiating the two cultivation regions. In addition, codonoside A and codonoside B, two characteristic glycosides of *Codonopsis*, also showed distinct concentration variations between CLC and CKT. Taken together, the regional variation observed in these metabolites may provide preliminary support for the use of metabolic profiles as potential chemical fingerprints for geographical discrimination, for exploring environment-related variation in bioactive constituents and for the development of chemometric classification models such as principal component analysis (PCA), partial least squares discriminant analysis (PLS-DA) and orthogonal partial least squares discriminant analysis (OPLS-DA).

Evaluation of the anti-inflammatory activity of *Codonopsis javanica* extracts

The NO production inhibition (%) and cell viability (%) are presented in Table 3. The negative control (1 % DMSO) exhibited no inhibitory effect on NO production while maintaining high cell viability (103.98 ± 0.84 %), confirming the non-cytotoxic nature of the experimental conditions. In contrast, stimulation with lipopolysaccharide (LPS, 1 µg/mL) markedly induced NO production

Table 3. *In vitro* anti-inflammatory activity of CKT-M and CLC-M samples

No	Sample	Sample concentration	NO production inhibition (%)	Cell viability (%)	IC_{50} value (µg/mL)
	Negative control (-) [DMSO]	1%	-	103.98 ± 0.84	-
	Positive control (+) [Cardamonin]	0.081	46.95 ± 1.23	86.77 ± 0.54	0.15
		0.81	87.98 ± 0.94	80.84 ± 0.63	
	LPS	1 µg/mL	0.0 ± 0.9	100.0 ± 0.13	-
1	CLC-M	256 µg/mL	82.02 ± 0.58	94.45 ± 0.56	98.22
		128 µg/mL	56.28 ± 0.17	98.54 ± 0.38	
		64 µg/mL	42.90 ± 0.45	99.14 ± 0.97	
2	CKT-M	256 µg/mL	86.93 ± 0.42	97.56 ± 0.98	84.69
		128 µg/mL	58.33 ± 0.94	99.59 ± 0.97	
		64 µg/mL	46.19 ± 1.03	100.99 ± 0.54	

NO: nitric oxide; DMSO: Dimethyl sulfoxide; LPS: Lipopolysaccharide; IC_{50}: half maximal inhibitory concentration.

without affecting cell viability, thereby validating the suitability of the inflammatory model. The positive control, cardamonin, demonstrated a concentration-dependent inhibition of NO production (46.95 ± 1.23 % at 0.081 µg/mL and 87.98 ± 0.94 % at 0.81 µg/mL), with an IC_{50} value of 0.15 µg/mL, confirming the reliability of the assay system.

The CKT-M exhibited an IC_{50} value of 84.69 µg/mL, which was lower than that of the CLC-M (98.22 µg/mL), indicating a stronger inhibitory effect on NO production. This difference may be associated with the higher abundance of phenolic compounds, including syringin, lobetyolin, catechol, tangshenoside I, codonoside A and codonoside B, in the CKT-M compared with the CLC-M. These compounds have been reported in previous studies to possess anti-inflammatory activity (47, 48).

Previous studies have suggested a potential relationship between these constituents and anti-inflammatory effects. For example, tangshenoside I and lobetyolin have been reported to exert anti-inflammatory activity by regulating key inflammatory mediators, including interleukin-6 (IL-6), interleukin-1β (IL-1β), tumor necrosis factor-α (TNF-α), myeloperoxidase (MPO) and nitric oxide (NO) (49). In addition, syringin has been shown to significantly reduce inflammatory cytokine levels in H9c2 cardiomyocytes subjected to H_2O_2-induced inflammation and oxidative stress (50). These findings support the hypothesis that the stronger NO inhibition observed for CKT-M is closely related to its higher content of these bioactive compounds. Furthermore, both extracts exhibited acceptable safety profiles, as indicated by cell viability values exceeding 80 % (51).

Evaluation of the phagocytosis-enhancing activity of *Codonopsis javanica* extract

Previous studies evaluating the immunomodulatory activity of *Codonopsis* extracts have commonly employed cyclophosphamide (CP)-induced immunosuppressed BALB/c mouse models and assessed immune function through immune organ indices, humoral and cellular immune parameters, cellular immune responses, as well as gut microbiota profiling using 16S rRNA gene sequencing (52). The activity was evaluated using an S180 tumor-bearing mouse model to investigate immunoenhancement accompanied by inhibition of tumor growth, with quantitative determination of cytokines and immune-related markers such as IL-2, IFN-γ and TNF-α (53), A solid H22 tumor–bearing mouse model was employed to evaluate the antitumor effects of the CPP-SeNPs complex via immune enhancement mechanisms. The evaluated parameters included serum cytokine expression, activities of immune cells (NK cells, macrophages and lymphocytes) and apoptotic markers in tumor cells to elucidate the *in vivo* mechanisms of action (54). To date, no reports have documented the use of the NBT reduction assay to evaluate the phagocytic activity of *Codonopsis* extracts. In the present study, this method was applied to preliminarily assess immunomodulatory activity by determining phagocytic capacity based on NBT reduction.

Based on the aforementioned method, the ability of the tested sample to stimulate macrophage cells and enhance phagocytic activity was evaluated (Table 4). The results suggest that show that the CLC-M and CKT-M sample induced phagocytic activity at a concentration of 100 µg/mL, reaching 15.39 ± 1.62 % and 17.25 ± 1.59 % with statistically significant differences compared with the control.

These results indicate that CKT-M exhibited a greater ability to induce phagocytic activity at a concentration of 100 µg/mL compared with CLC-M. This effect may be attributed to the higher contents of syringin, lobetyolin and tangshenoside I in the CKT-M sample than in CLC-M. Previous studies have demonstrated that syringin exhibits immunomodulatory activity by inhibiting classical complement-mediated immunohaemolysis and suppressing TNF-α production as well as CD8+ cytotoxic T-cell proliferation in a dose-dependent manner (55), while *Codonopsis* radix extracts and their

Table 4. Phagocytosis-stimulating activity of the tested samples

Concentration (µg/mL)	CKT-M		CLC-M	
	NBT reduction (%)	Cell survival (%)	NBT reduction (%)	Cell survival (%)
200	-1.37 ± 0.12	84.12 ± 3.45	-1.41 ± 0.42	84.22 ± 3.61
150	3.67± 0.25	86.03 ± 2.81	3.17± 0.18	85.15 ± 2.69
100	17.25* ± 1.59	95.27 ± 3.06	15.39* ± 1.62	94.68 ± 3.18
20	7.12 ± 0.54	98.64 ± 1.28	6.54 ± 0.68	99.17 ± 1.17
4	4.31 ± 0.29	100.78 ± 1.52	4.31 ± 0.29	101.24 ± 1.40
0.8	-2.83 ± 0.25	103.19 ± 3.04	-2.83 ± 0.25	102.72 ± 3.19

NBT: nitroblue tetrazolium; *$p < 0.05$ compared with the control group.

constituent compounds, particularly tangshenoside I and lobetyolin, possess immunostimulatory potential through enhancement of lymphocyte activation and function (56).

Conclusion

This study reveals significant regional differences in the chemical profiles and biological activities of *Codonopsis javanica* roots from Vietnam. Variations in chemical composition were associated with distinct anti-inflammatory and immunomodulatory activities, suggesting a close relationship between metabolite profiles and bioactivity. The integration of Ultra-performance liquid chromatography - Quadrupole Time-of-Flight - Tandem mass spectrometry (UPLC-QTOF-MS/MS)-based metabolite profiling with biological activity evaluation provides valuable scientific data for this medicinal plant. The findings further highlight the importance of ecological and climatic factors in influencing the quality of this medicinal plant. Based on the preliminary investigations, it is necessary to expand the sample size and further investigate the effects of growth conditions and processing on the quality of the medicinal material. In addition, multivariate statistical analyses should be applied to better elucidate the relationships among metabolite profiles, biological activities and the origin of the medicinal material.

Acknowledgements

The authors gratefully acknowledge the financial support provided by the Vietnam-China joint research project (Grant No. NĐT/CN/24/03), under which this work was performed.

Authors' contributions

HTT contributed to conceptualisation, methodology, writing of the original draft and structuring of the manuscript. NTP contributed to writing of the original draft, data analysis, formatting and revision. TTT contributed to writing of the original draft and data analysis. HC was responsible for reviewing and editing. DTTH contributed to methodology and data collection. LMH contributed to reviewing and editing, project administration and revision. All authors have read and approved the final manuscript.

Compliance with ethical standards

Conflict of interest: Authors do not have any conflict of interests to declare.

Ethical issues: None

Declaration of generative AI and AI-assisted technologies in the writing process

During the preparation of this work the authors used ChatGPT (OpenAI) solely for language editing. After using this tool/service, the authors reviewed and edited the content as needed and takes full responsibility for the content of the publication.

References

1. Nguyen TQ, Dam KH, Bui TT, Ngo TL, Nguyen DT, To HA, et al. Quantification of total saponins and polysaccharides in *Codonopsis* (Dang sam) collected from Sung Trai – Ha Giang. Vietnam Med J. 2022;513(1):163–67. https://doi.org/10.51298/vmj.v513i1.2357
2. Nguyen TBN, Dinh TNH, Le NN. An investigation and analysis of features of *Codonopsis javanica* (Blume) Hook.f. & Thoms in Son La. Int J Hortic Agric Food Sci. 2022;6(5):7–12. https://doi.org/10.22161/ijhaf.6.5.2
3. Nguyen PTN, Nguyen DV, Le VTT, Than TMP, Long GB, Tran QT. Instant tea from Codonopsis javanica L. root extract via spray drying. Foods Raw Mater. 2020;8(2):385–91. https://doi.org/10.21603/2308-4057-2020-2-385-391
4. Li H, Song Y, Shi X, Ma B, Yao Y, Li H, et al. Study on the correlation between major medicinal constituents of *Codonopsis pilosula* during its growth cycle and ecological factors and determination of optimal ecological factor ranges. Agronomy. 2025;15(5):1057. https://doi.org/10.3390/agronomy15051057
5. Liu X, Chen Z, Wang X, Luo W, Yang F. Quality assessment and classification of *Codonopsis* radix based on fingerprints and chemometrics. Molecules. 2023;28(13):5127. https://doi.org/10.3390/molecules28135127
6. Chen QF, Deng XY, Zhu HF. Determination of lobetyolin and syringin in *Codonopsis* radix from different places by HPLC. Sci Technol Food Ind. 2016;(06):64–67. https://doi.org/10.13386/j.issn1002-0306.2016.06.004
7. Qiao CF, He ZD, Han QB, Xu HX, Jiang RW, Li SL, et al. The use of lobetyolin and HPLC-UV fingerprints for quality assessment of radix *Codonopsis*. J Food Drug Anal. 2007;15(3):258–64. https://doi.org/10.38212/2224-6614.2408
8. Wang SS, Zhang T, Wang L, Dong S, Wang DH, Li B, et al. The dynamic changes in the main substances in *Codonopsis pilosula* root provide insights into the carbon flux between primary and secondary metabolism during different growth stages. Metabolites. 2023;13(3):456. https://doi.org/10.3390/metabo13030456
9. Xu L, Ma L, Chen G, Wei R, Ma Y, Dang J, et al. Mechanisms of pathogenic microorganisms, root antioxidant systems and secondary metabolites of *Codonopsis pilosula* (Franch.) Nannf. in response to continuous cropping obstacles. Ind Crops Prod. 2025;225:120455. https://doi.org/10.1016/j.indcrop.2025.120455
10. Wen L, Wang Y, Song P, Wang Z, Tang Z, Guo Y, et al. Exploration of postharvest conditions for *Codonopsis pilosula* Nannf. var. modesta (Nannf.) L. T. Shen roots based on sensory quality, active components, antioxidant capacity and physiological changes at different storage temperatures. Foods. 2023;12(24):4418. https://doi.org/10.3390/foods12244418
11. Hoang DN, Vu TT, Le DQ, Do TH, Tran TT, Bui TT, et al. Study on chemical constituents and antifungal activity of *Codonopsis pilosula* roots. J Chem Biol Phys Sci. 2020;25(2):65–70.
12. Tran H, Ma TBT, Nguyen P, Nguyen TH, Bui BT, Phung PA, et al. Optimization of ultrasonic-assisted extraction parameters for saponins from *Codonopsis javanica* (Blume) Hook. f. roots cultivated in Tay Giang District, Quang Nam Province. Vietnam J Sci Technol. 2025;67(9). https://doi.org/10.31276/VJST.67(9).28-33
13. Mac XH, Ngo DAT. Isolation of saponins from *Codonopsis pilosula* (Franch.) Nannf. roots using enzyme-assisted and ultrasound-assisted extraction methods. Tra Vinh Univ J Sci. 2020;40:83.
14. Shah SMZ, Ramzan M, Khan MN, Shadab H, Usman M, Rahman S, et al. Untargeted screening of plant metabolites based on data-independent and data-dependent acquisition modes using LC-ESI-QTOF-MS: *Tribulus terrestris* L. as a case study. Arab J Chem. 2023;16:104978. https://doi.org/10.1016/j.arabjc.2023.104978
15. Hu Z, Yan M, Song C, Sato M, Su S, Lin S, et al. An integrated approach for the comprehensive characterization of metabolites in broccoli (*Brassica oleracea* var. italica) by liquid chromatography high-resolution tandem mass spectrometry. Plants. 2025;14(20):3223. https://doi.org/10.3390/plants14203223
16. Breaud C, Lallemand L, Mares G, Mabrouki F, Bertolotti M, Simmler

C, et al. LC-MS based phytochemical profiling towards the identification of antioxidant markers in some endemic Aloe species from Mascarene Islands. Antioxidants. 2023;12(1):50. https://doi.org/10.3390/antiox12010050

17. Persaud M, Lewis A, Kisiala A, Smith E, Azimychetabi Z, Sultana T, et al. Untargeted metabolomics and targeted phytohormone profiling of sweet aloes (*Euphorbia nerifolia*) from Guyana: an assessment of asthma therapy potential in leaf extracts and latex. Metabolites. 2025;15(3):177. https://doi.org/10.3390/metabo15030177
18. Tsugawa H, Cajka T, Kind T, Ma Y, Higgins B, Ikeda K, et al. MS-DIAL: data independent MS/MS deconvolution for comprehensive metabolome analysis. Nat Methods. 2015;12(6):523–26. https://doi.org/10.1038/nmeth.3393
19. Rivera-Pérez A, Garrido Frenich A. Comparison of data processing strategies using commercial vs. open-source software in GC-Orbitrap-HRMS untargeted metabolomics analysis for food authentication: thyme geographical differentiation and marker identification as a case study. Anal Bioanal Chem. 2024;416 (18):4039–55. https://doi.org/10.1007/s00216-024-05347-0
20. Ministry of Health. Vietnamese Pharmacopoeia. 5th ed. Vol. 2. Hanoi: Medical Publishing House; 2017. p. 1156–57.
21. Pham HH. An illustrated flora of Vietnam. Ho Chi Minh City: Tre Publishing House. 2000;3:101.
22. Jia Y, Jin T. Enhancement of bioactive compounds and antioxidant properties in *Codonopsis pilosula* through extrusion processing and development of *Codonopsis*-oat powder. Foods. 2024;13(20):3485. https://doi.org/10.3390/foods13203485
23. Nam M, Jo SR, Kim YC, Kim MS. UPLC-QTOF-MS-based metabolomics and antioxidant capacity of *Codonopsis lanceolata* from different geographical origins. Foods. 2023;12(2):267. https://doi.org/10.3390/foods12020267
24. Geng L, Zhang Q, Li Q, Zhang Q, Wang C, Song N, et al. Fucoidan from the cell wall of *Silvetia siliquosa* with immunomodulatory effect on RAW 264.7 cells. Carbohydr Polym. 2024;332:121883. https://doi.org/10.1016/j.carbpol.2024.121883
25. Dirsch VM, Stuppner H, Vollmar AM. The Griess assay: suitable for a bio-guided fractionation of anti-inflammatory plant extracts? Planta Med. 1998;64(5):423–26. https://doi.org/10.1055/s-2006-957473
26. Aldridge C, Razzak A, Babcock TA, Helton WS, Espat NJ. LPS-stimulated RAW 264.7 macrophage inducible nitric oxide synthase (iNOS) and nitric oxide production is decreased by an omega-3 fatty acid lipid emulsion. J Surg Res. 2008;149(2):296–302. https://doi.org/10.1016/j.jss.2007.12.758
27. Manosroi A, Saraphanchotiwitthaya A, Manosroi J. In vitro immunomodulatory effect of *Pouteria cambodiana* (Pierre ex Dubard) Baehni extract. J Ethnopharmacol. 2005;101:90–94. https://doi.org/10.1016/j.jep.2005.03.031
28. Ozbalci C, Chiapparino A, Duban-Deweer S, Hachani J, Saint-Pol J, Baker PRS. The simultaneous processing of DDA and SWATH data by MS-DIAL software improves coverage for untargeted lipidomics analysis. SCIEX Tech Note. SCIEX. 2019.
29. Yuan F, Yan S, Zhao J. Elucidating the phytochemical landscape of leaves, stems, and tubers of *Codonopsis convolvulacea* through integrated metabolomics. Molecules. 2024;29(13):3193. https://doi.org/10.3390/molecules29133193
30. Chang YK, Kim SY, Han BH. Chemical studies on the alkaloidal constituents of Codonopsis *lanceolata*. Yakhak Hoeji. 1986;30(1):1–7.
31. Yang X, Zhu HF, Wang T, Chen QF, Wan D, Peng R. Comparative analysis of amino acid composition and nutritional value of roots of *Codonopsis pilosula* from Wushan and other growing regions in China. Food Sci. 2014;35(15):251–55.
32. Zhao Q, Wu YN, Fan Q, Han QQ, Paré PW, Xu R, et al. Improved growth and metabolite accumulation in *Codonopsis pilosula* (Franch.) Nannf. by inoculation of Bacillus amyloliquefaciens GB03. J Agric Food Chem. 2016;64(41):8103–08. https://doi.org/10.1021/acs.jafc.6b03390
33. Wang P, Liu F, Zhang D, Peng J, Liu S, Wu F. Quality evaluation of *Codonopsis pilosula* in China. Chin J Pharm. 2024;59(23):2226–40. https://doi.org/10.11669/cpj.2024.23.004
34. Nguyen HTP, Nguyen TDT, Nguyen TTH, Pham VH, Nguyen HHD, Tran THH, et al. Polyacetylene and phenolic constituents from the roots of *Codonopsis javanica*. Nat Prod Res. 2022;36(9):2314–20. https://doi.org/10.1080/14786419.2020.1833200
35. Yang C, Gou Y, Chen J, An J, Chen W, Hu F. Structural characterization and antitumor activity of a pectic polysaccharide from *Codonopsis pilosula*. Carbohydr Polym. 2013;98(1):886–95. https://doi.org/10.1016/j.carbpol.2013.06.079
36. Guo X, Yang R, Wang Y, Wang J, Wang Y, Zou H, et al. Prediction of chemical composition and sensory information of *Codonopsis* radix based on electronic nose. Molecules. 2025;30(5):1146. https://doi.org/10.3390/molecules30051146
37. Ma XQ, Leung AKM, Chan CL, Su T, Li WD, Li SM, et al. UHPLC UHD Q-TOF MS/MS analysis of the impact of sulfur fumigation on the chemical profile of *Codonopsis* radix (Dangshen). Analyst. 2014;139:505–16. https://doi.org/10.1039/C3AN01561K
38. Koo SC, Kim HW, Kim JW, Kim YS, Kim JY, Kim JH, et al. Discovery and characterization of chemical compounds that inhibit the function of bacterial neuraminidase from *Codonopsis ussuriensis*. Appl Sci. 2022;12(12):6254. https://doi.org/10.3390/app12126254
39. Xu Z, Cai R, Chai H, Chen S, Liang Y, Li X, et al. Simultaneous quantification of 66 compounds in two Tibetan *Codonopsis* species reveals four chemical features by database-enabled UHPLC-Q-Orbitrap-MS/MS analysis. Molecules. 2024;29(21):5203. https://doi.org/10.3390/molecules29215203
40. Dong J, Na Y, Hou A, Zhang S, Yu H, Zheng S, et al. A review of the botany, ethnopharmacology, phytochemistry, analysis method and quality control, processing methods, pharmacological effects, pharmacokinetics and toxicity of *Codonopsis* radix. Front Pharmacol. 2023;14:1162036. https://doi.org/10.3389/fphar.2023.1162036
41. Zhang J, Xu W, Wang P, Huang J, Bai JQ, Huang ZH, et al. Chemical analysis and multi-component determination in Chinese medicine preparation Bupi Yishen formula using ultra-high performance liquid chromatography with linear ion trap-Orbitrap mass spectrometry and triple-quadrupole tandem mass spectrometry. Front Pharmacol. 2018;9:568. https://doi.org/10.3389/fphar.2018.00568
42. Nguyen HHT, Nguyen TDT, Nguyen NTH, Pham VH, Nguyen HHD, Tran THH, et al. Codojavanosides A–C, three new sesquiterpenoid glycosides from the roots of *Codonopsis javanica*. Phytochem Lett. 2020;40:166–70. https://doi.org/10.1016/j.phytol.2020.10.002
43. Li M, He Y, Chen C, Liu L, Xu J, Cao J, et al. Ecological factors drive the accumulation of active components in *Codonopsis pilosula*. Phyton (Int J Exp Bot). 2025;94(8):2575–91. https://doi.org/10.32604/phyton.2025.064518
44. General Statistics Office of Vietnam. Administrative Unit and Climate. https://tinyurl.com/ywpy3tnk
45. Trinh PT. Study on the characteristics of land use of basaltic red soils (Ferralsols) in Dak Lak province. Sci Technol Dev J. 2012;10 (7):1024–31.
46. Wang Z, Jia Y, Li P, Tang Z, Guo Y, Wen L, et al. Study on environmental factors affecting the quality of *Codonopsis* radix based on MaxEnt model and all-in-one functional factor. Sci Rep. 2023;13:20726. https://doi.org/10.1038/s41598-023-46546-6
47. Zhang A, Liu Z, Sheng L, Wu H. Protective effects of syringin against lipopolysaccharide-induced acute lung injury in mice. J Surg Res. 2017;209:252–57. https://doi.org/10.1016/j.jss.2016.10.027
48. Ren J, Lin Z, Yuan Z. Tangshenosides from *Codonopsis lanceolata* roots. Phytochem Lett. 2013;6:567–69. https://doi.org/10.1016/j.phytol.2013.07.006

49. Chen Q, Sun Y, Hu X, Xie Q, Liu W, Lei J, et al. The effect and mechanism of *Codonopsis* radix and its active components tangshenoside I and lobetyolin on preventing gastric ulcer based on spectrum-effect relationship. J Ethnopharmacol. 2025;353(Pt A):120281. https://doi.org/10.1016/j.jep.2025.120281

50. Zhao D, Liu K, Wang J, Shao H. Syringin exerts anti-inflammatory and antioxidant effects by regulating SIRT1 signaling in rat and cell models of acute myocardial infarction. Immun Inflamm Dis. 2023;11 (2):e775. https://doi.org/10.1002/iid3.775

51. Wongwat T, Srihaphon K, Pitaksutheepong C, Boonyo W, Pitaksuteepong T. Suppression of inflammatory mediators and matrix metalloproteinase (MMP)-13 by *Morus alba* stem extract and oxyresveratrol in RAW 264.7 cells and C28/I2 human chondrocytes. J Tradit Complement Med. 2019;10(2):132–40. https://doi.org/10.1016/j.jtcme.2019.03.006

52. Fu YP, Feng B, Zhu ZK, Feng X, Chen SF, Li LX, et al. The polysaccharides from *Codonopsis pilosula* modulate the immunity and intestinal microbiota of cyclophosphamide-treated immunosuppressed mice. Molecules. 2018;23(7):1801. https://doi.org/10.3390/molecules23071801

53. Fan Y, Long Y, Gong Y, Gao X, Zheng G, Ji H. Systemic immunomodulatory effects of *Codonopsis pilosula* glucofructan on S180 solid-tumor-bearing mice. Int J Mol Sci. 2023;24(21):15598. https://doi.org/10.3390/ijms242115598

54. Wu L, Peng M, Jing Y, Yang X, Yang J. Immunomodulatory effect of polysaccharides from the extraction of *Codonopsis javanica* (Blume) Hook. f. et Thomson (Campanulaceae) roots in female rats. Nat Prod Res. 2021;35(24):5883–87. https://doi.org/10.1080/14786419.2020.1800694

55. Cho JY, Nam KH, Kim AR, Park J, Yoo ES, Baik KU, et al. *In vitro* and in vivo immunomodulatory effects of syringin. J Pharm Pharmacol. 2001;53(9):1287–94. https://doi.org/10.1211/0022357011776577

56. Liu J, Wang Y, Li B, Qi Y, Wei X, Liu H, et al. The effective approach for the quality control of *Codonopsis* radix based on quality markers of immune activity. J Sep Sci. 2022;45(7):1539–50. https://doi.org/10.1002/jssc.202100829

Additional information

Peer review: Publisher thanks Sectional Editor and the other anonymous reviewers for their contribution to the peer review of this work.

Reprints & permissions information is available at https://horizonepublishing.com/journals/index.php/PST/open_access_policy

Publisher's Note: Horizon e-Publishing Group remains neutral with regard to jurisdictional claims in published maps and institutional affiliations.

Indexing: Plant Science Today, published by Horizon e-Publishing Group, is covered by Scopus, Web of Science, BIOSIS Previews, Clarivate Analytics, NAAS, UGC Care, etc
See https://horizonepublishing.com/journals/index.php/PST/indexing_abstracting

Copyright: © The Author(s). This is an open-access article distributed under the terms of the Creative Commons Attribution License, which permits unrestricted use, distribution and reproduction in any medium, provided the original author and source are credited (https://creativecommons.org/licenses/by/4.0/)

Publisher information: Plant Science Today is published by HORIZON e-Publishing Group with support from Empirion Publishers Private Limited, Thiruvananthapuram, India.